Journal of Earth Science, *Vol. 25*, *No. 5*, *p. 895–900*, *October 2014* *ISSN 1674-487X*
Printed in China
DOI: 10.1007/s12583-014-0475-x

The Use of Ground Penetrating Radar for Mapping Rock Stratigraphy and Tectonics: Implications for Geotechnical Engineering

Awni T Batayneh*, **Taisser Zumlot**, **Habes Ghrefat**, **Mahmud M El-Waheidi**, **Yousef Nazzal**
Department of Geology and Geophysics, *King Saud University*, *PO Box* 2455, *Riyadh* 11451, *Saudi Arabia*

ABSTRACT: This paper presents results from ground penetrating radar surveys using the SIR-10B GPR instrument (manufactured by Geophysical Survey System Inc., USA), with 400 MHz monostatic antenna (model 5 103). Survey was made over 3 excavation levels along the highway section at the Ras en Naqab escarpment area, Southwest Jordan. A total of 217 m along 4 profiles were covered in the winter of 2012. The objectives of the study are (i) to evaluate the resolution of the GPR technique in the field for detecting and locating anomalies caused by subsurface structures like cavities, fractures and faults, and (ii) to describe stratigraphic nomenclature of the subsurface rocks of the area. 2D interpretation of the obtained data and the geological information demonstrate a strong correlation between the GPR anomalies and the subsurface geology. Based upon the lateral and vertical velocity changes with depth, the thickness and orientation of the subsurface layers are outlined. Analysis of the exposed section shows good agreement between the estimated thicknesses of lithostratigraphic units and the quantitative assessment of the radar waves velocity inferred from GPR data.
KEY WORDS: ground penetrating radar, rock stratigraphy, rock tectonics, Ras en Naqab, Jordan.

1 BACKGROUND

Jordan is located on the northwestern edge of the Arabian Plate and has an area of about 96 000 km^2 (Fig. 1a). The landscape of Jordan is a fast semi-desert to desert plateau in the east. To the west is a mountainous region rising to a height of 800 to more than 1 700 m above sea level. Between two mountainous areas west of Jordan and east of Israel lies a north-south striking Dead Sea rift (DSR). The rift escarpment separates drainage into the Dead Sea Basin, ~430 m below sea level, from drainage into the plateau interior. The east bank of the DSR is controlled by the regional tectonics of the horizontally, northward-moving Arabian Plate. Therefore, the compressed structures are folded with a higher intensity of deformation close to the rift fault and decrease eastwards, thus leading to deformational belts which represent potential zones of weakness, characterized by displacements and stress release represented by major landslides, joints, fractures, rock collapses, local earthquakes, rock movements and caverns. Recent studies focused on the regional tectonics of the DSR and surrounding area are of the work of Diabat (2002), Zain Eldeen et al. (2002) and Diabat et al. (2004). The relative motion across the DSR has been estimated by both regional plate motion models and local slip rate considerations. The regional plate motion studies use the fault orientation, additional local observations, and constraints from the motion of neighboring plates to estimate 5–10 mm/yr of relative motion across the DSR (Chu and Gordon, 1998; Joffe and Garfunkel, 1987). Local seismic studies yield a wider range of slip motion of 1 to 10 mm/yr (Klinger et al., 2000; Shapira and Hofstetter, 1993).

Central Jordan surface morphology is dominantly characterized by flat lying. Rugged topography associated with the Ras en Naqab escarpment separates the northern Jordanian limestone area from the southern basement complex (Fig. 1a). A difference in altitude between these two geologic-physiographic provinces is in the order of 600 m. The escarpment area strikes in a northwest-southeast direction. A modern highway connecting north via central Jordan to the south was constructed 30 years ago. Because of the rugged terrain in the Ras en Naqab escarpment and it is considerably higher construction cost, works on this highway ceased in this area. However, a site on the escarpment was excavated up to five terrace levels (I through V, Fig. 1b). Each level is about 200 m long, 4 m wide and about 6 m high. These terraces have an east-southeast to west-northwest alignment. Fresh cutting and excavation work at the sites revealed the presence of localized zones of underground shearing, strike-slip faults, erosional surfaces, paleochannels, slickensides and different types of structural deformation and near-surface fractures. Detection and location of these features has become one of the major tasks in road and building construction and maintenance (Batayneh and Al-Diabat, 2002; Batayneh and Al-Zoubi, 2000; Batayneh et al., 1999; Smith, 1986).

*Corresponding author: awni_batayneh@yahoo.com
© China University of Geosciences and Springer-Verlag Berlin Heidelberg 2014

Manuscript received December 18, 2013.
Manuscript accepted July 15, 2014.

Batayneh, A. T., Zumlot, T., Ghrefat, H., et al., 2014. The Use of Ground Penetrating Radar for Mapping Rock Stratigraphy and Tectonics: Implications for Geotechnical Engineering. *Journal of Earth Science*, 25(5): 895–900. doi:10.1007/s12583-014-0475-x

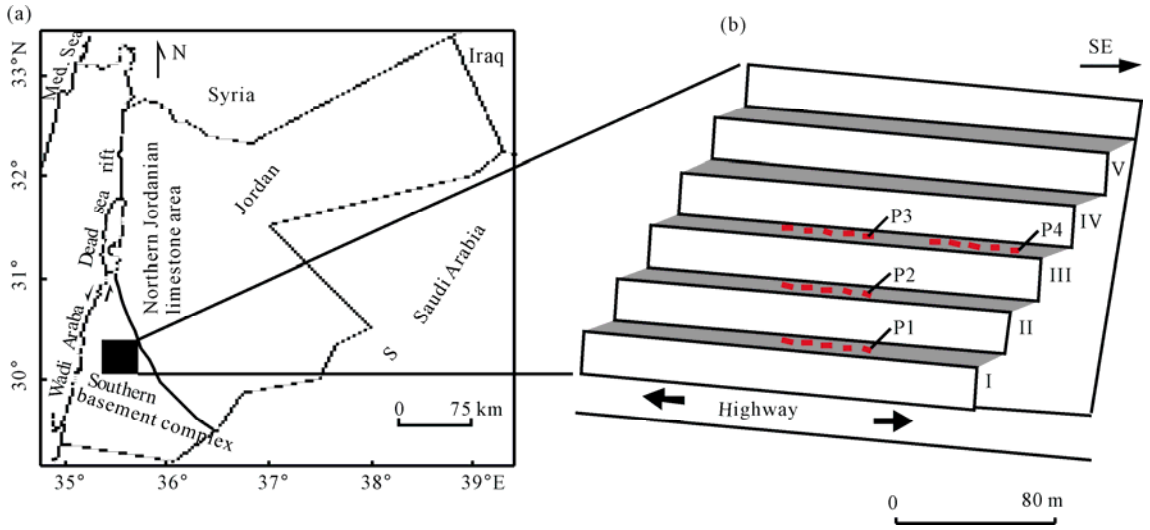

Figure 1. (a) Site map of the study area; (b) locations of the four GPR lines (P1–P4) in Ras en Naqab area.

From a geological point of view, and during the Late Cretaceous Period, a major transgression of the Tethys Ocean resulted into carbonate facies deposition of the Ajlun Group (Cenomanian–Turonian) throughout Jordan. The rocks of this group, which disconformably overlies the Kurnub sandstone group of Lower Cretaceous age (Barjous, 1995), consists of the Na'ur limestone (NL), the Fuheis/Hummer/Shueib (F/H/S), and the Wadi Es-Sir limestone (WSL) formations. The base of the Ajlun group comprises siltstones and mudstones up to 10 m thick. These members form a transitional zone at the base of the NL Formation. Generally, NL Formation contains three horizons; the upper and the lower consist of massive, hard carbonate units each up to 20 m thick (Batayneh and Barjous, 2003), while the strata interbedded between these units comprise alternating thin beds of marl, dolomite and sandstone. The overlying marl, limestone, dolomitic sandstone, siltstone-mudstone, claystone and sandstone beds are equivalent, in upward sequence, to the F/H/S formations (Cenomanian–Lower Turonian). At the studied site, these formations are about 50 m thick (Batayneh and Barjous, 2003). The WSL Formation of the Turonian age is about 100 m thick and dominantly consists of massive dolomitic limestone. At the base it is composed of massive sandy dolomitic carbonate beds intercalated with marly limestone, silty mudstone and nodules of chert. The upper part of this formation is composed of a massive to bedded sandy and dolomitic limestone. Figure 2 shows a stratigraphic column from the studied site (after Batayneh and Barjous, 2003).

In the present study, we present results of ground penetrating radar (GPR) technique application to investigate subsurface geology in terms of environmental and engineering application. The study was performed at the Ras en Naqab escarpment area, southwest Jordan, in the winter of 2012. This site has a large existing geological data base, and thus is ideal for GPR technique in detecting and locating potential geologic features.

2 GENERAL PRINCIPLES AND DATA ACQUISITION

GPR is an electromagnetic profiling technique utilized for high resolution mapping of subsurface features. GPR technique has been used in geological (e.g., Carrozzo et al., 2003; Nobes et al., 2001; McMechan et al., 1998), hydrological and hydrogeological studies (e.g., van Overmeeren, 1998; Beres and Haeni, 1991), in aquifers investigations (e.g., Arcone et al., 1998), water contamination (e.g., Benson, 1995; Daniels et al., 1995; Annan et al., 1991), geotechnical engineering (e.g., Batayneh et al., 2002; Barnhardt and Kayen, 2000; Birken and Versteeg, 2000; Saarenketo and Scullion, 2000), and in archeological investigations (e.g., Bonomo et al., 2009; Imai et al., 1987; Vaughan, 1986).

In the GPR technique, a short pulse of high frequency (10–1 000 MHz) electromagnetic energy is transmitted by the antennae through the ground surface and then receives its reflection from boundaries between layers or from internal irregularities of different electrical properties. The amount of energy that is reflected back to a radar antenna by an interface is dependent upon the contrast in the relative dielectric permittivity (Er) of the two layers. Abrupt boundaries that separate contrasting materials reflect more energy than gradual boundaries that separate materials with similar Er. The Er of soil materials is principally dependent upon moisture content (Buynevich and Fitzgerald, 2003; Annan et al., 1991; Beres and Haeni, 1991) and varies with temperature (phase-dependent), density, and antenna frequency (Denizman et al., 2010; Daniels, 2004). The reflection is detected on the surface, and the time between transmission and detection at the surface is proportional to depth. The depth of penetration of a GPR system is highly site specific and is limited by attenuation of the outgoing pulse. The velocity of the GPR is dependent on a degree of saturation and hence recent rainfall patterns. Generally, greater penetration is obtained in dry, sandy, and rocky soils and little penetration is obtained from moist, clayey conductive soils (Batayneh et al., 2002; Wolf et al., 1998; Liner and Liner, 1997; Cai et al., 1996).

The GPR survey layout at the Ras en Naqab site was constrained by GPR cable length and accessibility problems of the upper levels due to difficult terrain, so the lower three levels (I through III, Fig. 1b) were used for survey layout. A total of

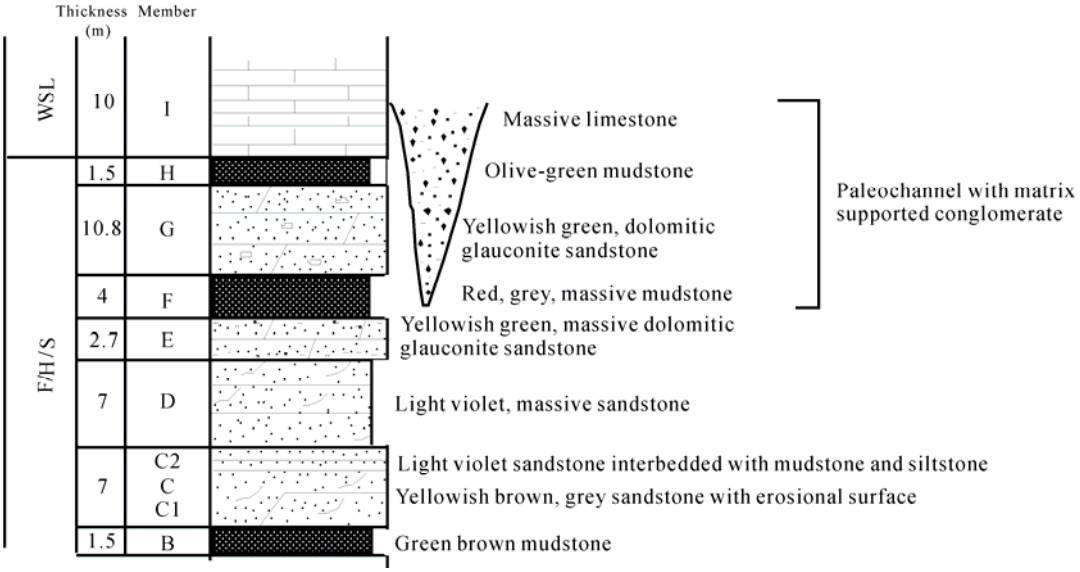

Figure 2. Measured geologic section at the Ras en Naqab site (after Batayneh and Barjous, 2003). F/H/S indicates Fu-heis/Hummer/Shueib formations (undifferentiated); WSL indicates Wadi Es-Sir limestone formation.

217 m along 4 profiles (P1–P4, Fig. 1b) were covered by GPR survey in the winter of 2012. Surveys were conducted using a SIR-10B GPR instrument, manufactured by Geophysical Survey System Inc. (GSSI), USA, with 400 MHz monostatic antenna (model 5 103). The antenna of this instrument combines the transmitter and receiver in a single housed system. Data were recorded at a speed of 50 scans/s, 5 m trace interval using odometer with a time window of 60 ns and 512 samples/s using a 16 bits A/D conversion and then digitally recorded on an internal hard disk drive. The gains, which is used to compensate for amplitude variations in the GPR image; early and late signals arrival times, were set relatively high to maximize a chance of anomalies detection of anomalies directly from the plots. The loss of signal amplitude is related to geometric spreading as well as intrinsic attenuation (Knight, 2001; Endres et al., 2000).

Velocity analysis of the subsurface units is based on the velocity spectrum technique, which is obtained by the stacking velocity to each reflector. It maps the *T*-*X* data of a single common midpoint (CMP) gather onto the velocity spectrum plane. The velocity analysis spectrum method was conducted using the GSSI RADAN version 5.0 software package. The accuracy of the velocity estimated by spectrum analysis is influenced by different factors: (i) depth and dip of the reflectors; (ii) spread length; (iii) signal/noise ratio; (iv) number of traces; and (v) static corrections. Works related to this technique are that of Taner and Koehler (1969), Yilmaz (1987), Mulder and ten Kroode (2002) and van Leeuwen and Mulder (2008).

A data set from 15 m long GPR line P3 (for location, see Fig. 1b) was chosen to illustrate the velocity spectrum technique (Fig. 3a). Using the RADAN software, an input of all the required parameters (i.e., interval distance, offset and minimum and maximum velocity values expected at the site) has been made and stacked amplitude for analysis was chosen. The estimated velocity of the subsurface layers is presented in Fig. 3b. Velocity analysis of the studied site with the help of GPR technique has been done by adopting the following procedure. The radar measurements were made over known subsurface rock units and structures, where the bedding attitudes gently dip ~25° to the W-NW, and the profile lengths are relatively small.

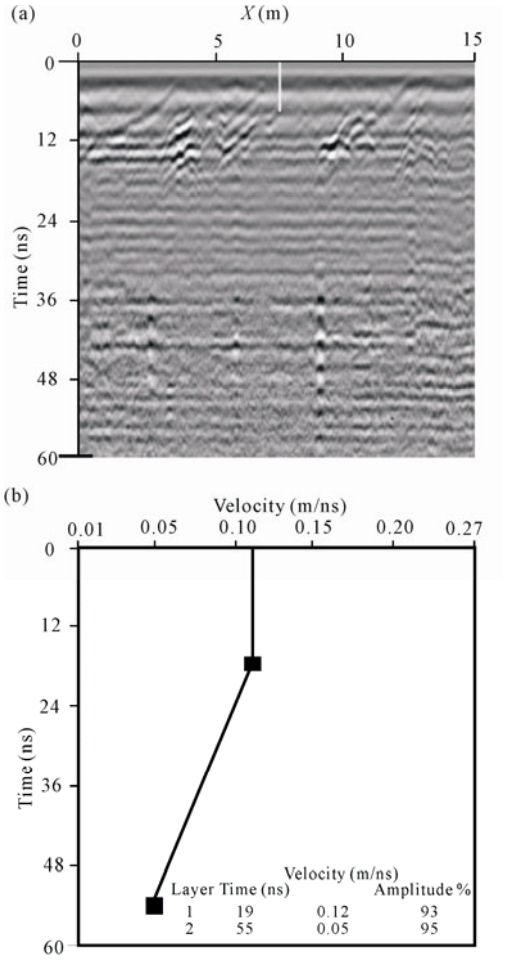

Figure 3. Velocity analysis using GPR survey. (a) Data set; (b) velocity analysis showing results of computation.

3 RESULTS AND DISCUSSION

Analysis of the GPR datasets from the measured profiles resulted into two-dimensional (2D) models revealing a detailed lithostratigraphic section (Fig. 2). The maximum depth of recognizable reflector under the studied site is about 3 m in general. Figure 4 shows the interpreted 2D section (400 MHz GPR) with geology superimposed on the velocity values for levels III (Fig. 4a), II (Fig. 4b), and I (Fig. 4c). Based on the interpretation of the obtained data, a geological section (Fig. 5) is constructed by grouping similar velocity values and using field based knowledge of the studied sequence exposed in the area (Fig. 2).

The base of the measured section, which consists of green-brown mudstone (Fig. 2, member B), shows a velocity value of 0.06 m/ns with a thickness of 1.5 m. The low velocity observed for this section is due to the presence of clay sub-horizons. Member C (Fig. 2) is about 7 m thick. It is dominated by 1.5 m thick yellowish brown, grey sandstone beds at the base and overlain by a sequence of light violet sandstone intercalated with mudstone and siltstone. These two units are marked as C1 and C2 on Fig. 2. Unit C1 shows a velocity value of 0.13 m/ns, while C2 shows a velocity value of 0.07 m/ns. Low velocity value from C2 may be due to the presence of siltstone with high moisture content.

The overlying member D (Fig. 2) is dominated by light violet massive sandstone. The determined velocity for this horizon is 0.16 m/ns and the thickness is about 2.5 m. The overlying member E, which consists of yellowish green glauconite sandstone with clay intercalation, shows a velocity value of 0.11 m/ns and a thickness of 2.7 m. A moderate velocity observed for this horizon is due to the presence of clay minerals. Member F, which is 4 m thick, consists of red, grey massive mudstone having a velocity value of 0.14 m/ns. The overlying sequence member G, comprises 10.8 m thick yellowish green sandstone with clay intercalations. The velocity for this sequence is 0.082 m/ns. The member H, a 1.5 m thick layer of olive-green mudstone with clay intercalations, has a velocity value of 0.05 m/ns. The low observed velocity for this member is due to the presence of mudstone and high moisture content.

The base of the WSL formation, member I (Fig. 2), comprises massive limestone interbedded with thin beds of mudstone. The measured thickness for this member is about 10 m. Along the measured GPR line P3 (Fig. 4a), only 2.5 m basal part of this horizon is present in the NW part, having a velocity value of 0.12 m/ns.

The 2D section (Fig. 4) shows rapid lateral velocity variations along the surveyed lines. Taking into consideration the lateral heterogeneities as evident in the GPR model section and field based geological observation of the exposed sections, two sub-parallel faults are interpreted by forming a horst-like structure (Fig. 5). These fault planes dip about 60 to 70 degrees to the SE and NW, respectively. Vertical offset along the faults varies from 12 m for the NW-dipping fault to 5 m for the SE-dipping faults (Fig. 5). A third minor fault, trending N16W, is also recognized (Fig. 5). The inferred fault has a vertical displacement of about 1 m. Figure 6 shows the geology and structure of the studied area.

Figure 7 shows a 2D interpreted GPR section with geology for the measured line P4 (for location, see Fig. 1b). The most prominent feature along the GPR line P4 (Fig. 7) is a series of reflections and diffractions at a profile distance between 29 and 46 m, interpreted to outline a filled paleochannel having a velocity value of 0.061 m/ns. This is visible to be discriminated from the surrounding sandstone bed (G member)

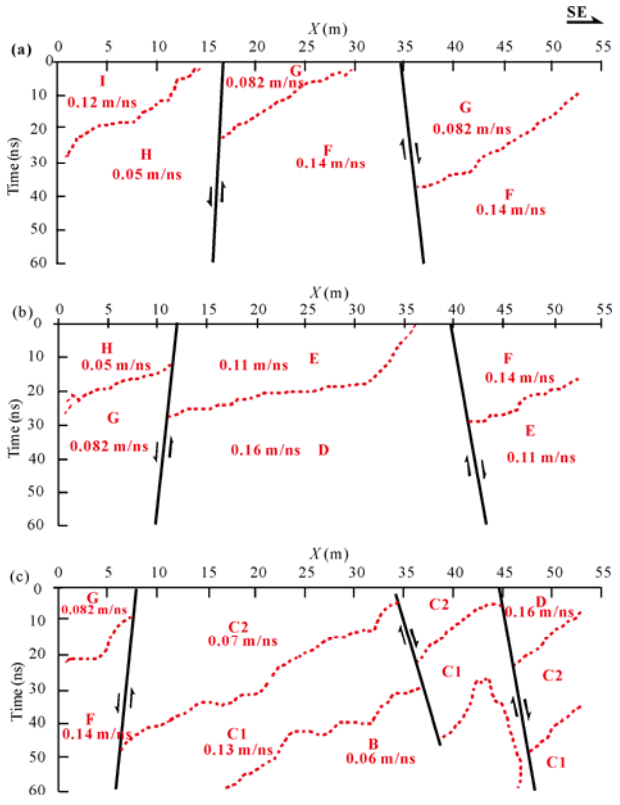

Figure 4. The interpreted 400 MHz GPR sections with geological setting for GPR lines P3 (a), P2 (b) and line P1 (c). Dashed lines represent rock unit boundary. Solid lines indicate fault.

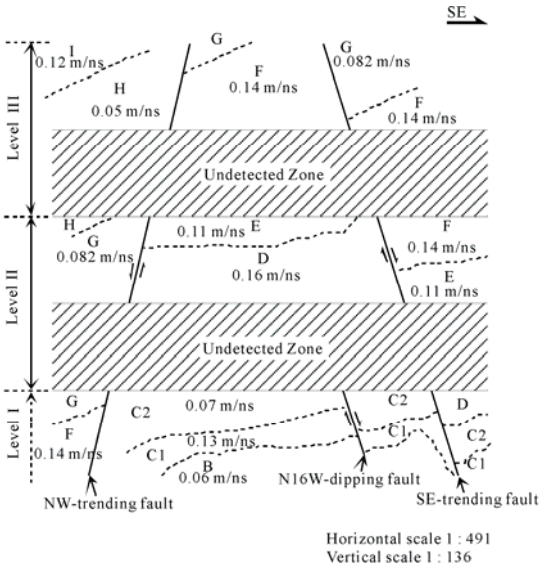

Figure 5. A 2D model constructed using the groups of similar velocity values and the geological information from the exposed section in the study area.

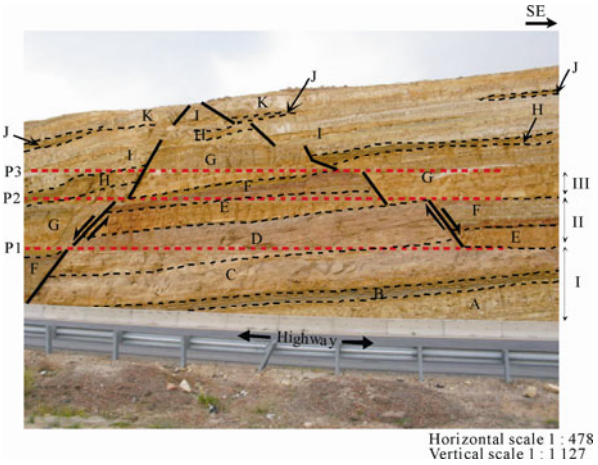

Figure 6. North-northeast trending photography with geological sequence members at the studied site.

Figure 8. North-northeast trending photography showing the geologic sequence and paleochannel at the site.

that have a velocity value of 0.082 m/ns and from the underlying massive mudstone (F member) that have a velocity value of 0.14 m/ns (Fig. 7). Diffractions at the right and left sides as well as below this feature are also visible (Fig. 7). These diffractions could have originated from cracks or fractures linking the surface. The geometry of the paleochannel is conical in shape (Fig. 8). Field evidence indicates that the sediment fill within the channel consists of grain supported conglomerate, with rock fragments up to 0.7 m in diameter (Batayneh and Barjous, 2003). The rock fragments are mostly derived from the F/H/S rocks, which consist of sandstone, mudstone, siltstone and marl. The matrix consists of sandstone and calcearenite.

4 CONCLUSIONS

In some geologic settings, GPR is a reliable, rapid, and economical geophysical technique for mapping shallow subsurface sediments and assessing structural and tectonic features. The thickness of the sediments can be reliably mapped where subsurface geology is not too complex and changes in subsurface velocity are associated with lithological changes.

Application of GPR technique to a site located in the Ras en Naqab area (South Jordan) proved helpful in mapping subsurface geology at shallow depths. Based upon the lateral and vertical velocity changes, thickness and slope of the subsurface lithological members are outlined. Thickness and lithology of the exposed section observed in the field are very much in agreement with these inferred from the GPR velocity data.

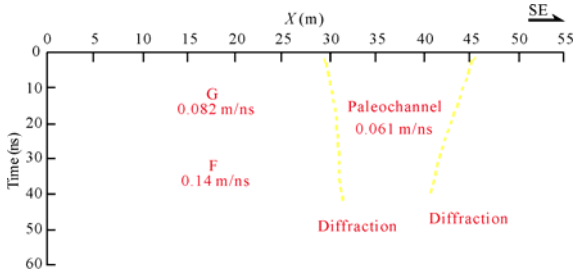

Figure 7. GPR section (400 MHz) from line P4 showing filled paleochannel.

The GPR data also demonstrated a reliable detection of shallow faults that coincide with geological features observed in the study area. The offset and dip of the faults also correlate well.

Paleochannel detection is another challenging problem in geophysical exploration that requires good resolution and depth penetration. GPR can be a successful method in detecting near-surface channels if the host rocks have different physical properties. Application of GPR in the study area provided useful information about the location and depth of the conglomerates filled paleochannels.

ACKNOWLEDGMENTS

The authors would like to extend their sincere appreciation to the Deanship of Scientific Research at King Saud University for its funding this research work. The authors thank sincerely a support received from the Natural Resources Authority of Jordan to accomplish this work. The two anonymous reviewers and the editorial of Journal of Earth Science had suggested their constructive comments to improve the article. The authors are thankful to them.

REFERENCES CITED

Annan, A. P., Bauman, P., Greenhouse, J., et al., 1991. Geophysics and DNAPLs. *Groundwater Management*, 5: 963–977

Arcone, S., Lawson, D. L., Delaney, A. J., et al., 1998. Ground-Penetrating Radar Reflection Profiling of Groundwater and Bedrock in an Area of Discontinuous Permafrost. *Geophysics*, 63: 1573–1584

Barjous, M., 1995. Geological Map of Petra and Wadi Al Lahyana. Map Sheet Nos. 3050 I and 3050 IV. Geological Mapping Division, Natural Resources Authority, Jordan

Barnhardt, W., Kayen, R., 2000. Radar Structure of Earthquake-Induced, Coastal Landslides in Anchorage, Alaska. *Environmental Geosciences*, 7: 38–45

Batayneh, A., Abueladas, A., Moumani, K., 2002. Use of Ground-Penetrating Radar for Assessment of Potential Sinkhole Conditions: An Example from Ghor al Haditha Area, Jordan. *Environmental Geology*, 41: 977–983

Batayneh, A. T., Al-Diabat, A. A., 2002. Application of 2D Electrical Tomography Technique for Investigating Landslides along

Amman-Dead Sea Highway, Jordan. *Environmental Geology*, 42: 399–403

Batayneh, A. T., Al-Zoubi, A. S., 2000. Detection of a Solution Cavity Adjacent to a Highway in Southwest Jordan Using Electrical Resistivity Methods. *Journal of Environmental and Engineering Geophysics*, 5: 25–30

Batayneh, A. T., Barjous, M. O., 2003. A Case Study of Dipole-Dipole Resistivity for Geotechnical Engineering from the Ras en Naqab Area, South Jordan. *Journal of Environmental and Engineering Geophysics*, 8: 31–38

Batayneh, A. T., Haddadin, G. S., Toubasi, U. M., 1999. Using the Head-on Resistivity Method for Shallow Rock Fracture Investigations, Ajlun, Jordan. *Journal of Environmental and Engineering Geophysics*, 4: 179–184

Benson, A., 1995. Application of Ground Penetrating Radar in Assessing Some Geological Hazards: Examples of Groundwater Contamination, Faults, Cavities. *Journal of Applied Geophysics*, 33: 177–193

Beres, M., Haeni, F., 1991. Application of Ground-Penetrating Radar Methods in Hydrogeologic Studies. *Ground Water*, 29: 375–386

Birken, R., Versteeg, R., 2000. Use of Four-Dimensional Ground Penetrating Radar and Advanced Visualization Methods to Determine Subsurface Fluid Migration. *Journal of Applied Geophysics*, 43: 215–226

Bonomo, N., Cedrina, L., Osella, A., et al., 2009. GPR Prospecting in a Prehispanic Village, NW Argentina. *Journal of Applied Geophysics*, 67: 80–87

Buynevich, I. V., Fitzgerald, D. M., 2003. High-Resolution Subsurface (GPR) Imaging and Sedimentology of Coastal Ponds, Maine, USA: Implications for Holocene Back-Barrier Evolution. *Journal of Sedimentary Research*, 73: 559–571

Cai, J., McMechan, G., Fisher, M., 1996. Application of Ground-Penetrating Radar to Investigation of Near-Surface Fault Properties in the San Francisco Bay Region. *Bulletin of Seismological Society of America*, 86: 1459–1470

Carrozzo, M. T., Leucci, G., Negri, S., et al., 2003. GPR Survey to Understand the Stratigraphy at the Roman Ships Archaeological Site (Pisa, Italy). *Archaeological Prospection*, 10: 57–72

Chu, D., Gordon, R. G., 1998. Current Plate Motions across the Red Sea. *Geophysical Journal International*, 135: 313–328

Daniels, D. J., 2004. Ground Penetrating Radar. 2nd Edition, The Institute of Electrical Engineers, London. 760

Daniels, J., Roberts, R., Vendl, M., 1995. Ground Penetrating Radar for the Detection of Liquid Contaminants. *Journal of Applied Geophysics*, 33: 195–207

Diabat, A., 2002. Strain Analysis of the Cretaceous Rocks in the Eastern Margin of the Dead Sea Transform, Jordan. *Dirasat*, 29: 159–172

Diabat, A. A., Atallah, M., Salih, M. R., 2004. Paleostress Analysis of the Cretaceous Rocks in the Eastern Margin of the Dead Sea Transform. *Journal of African Earth Sciences*, 38: 449–460

Denizman, C., Brevik, E. C., Doolittle, J., 2010. Ground-Penetrating Radar Investigation of a Rapidly Developed Small Island in a Lake in Southern Georgia, USA. *Journal of Cave and Karst Studies*, 72: 94–99

Endres, A. L., Clement, W. P., Rudolph, D. L., 2000. Ground Penetrating Radar Imaging of an Aquifer during a Pumping Test. *Ground Water*, 38: 566–76

Imai, T., Sakayama, T., Kanemori, T., 1987. Use of Ground-Probing Radar and Resistivity Surveys for Archaeological Investigations. *Geophysics*, 52: 137–150

Joffe, S., Garfunkel, Z., 1987. Plate Kinematics of the Circum Red Sea. Are Evaluation. *Tectonophysics*, 141: 5–22

Klinger, Y., Avouac, J. P., Abou Karaki, N., et al., 2000. Slip Rate on the Dead Sea Transform Fault in Northern Araba Valley. *Geophysical Journal International*, 142: 755–768

Knight, R., 2001. Ground Penetrating Radar for Environmental Applications. *Annual Review of Earth and Planetary Sciences*, 29: 229–255

Liner, C., Liner, J., 1997. Application of GPR to a Site Investigation Involving Shallow Faults. *Leading Edge*, 16: 1649–1651

McMechan, G. A., Louks, R., Zeng, X., et al., 1998. Ground Penetrating Radar Imaging of a Collapsed Paleocave System in the Ellenburger Dolomite, Central Texas. *Journal of Applied Geophysics*, 39: 1–10

Mulder, W. A., ten Kroode, A. P. E., 2002. Automatic Velocity Analysis by Differential Semblance Optimization. *Geophysics*, 67: 1184–1191

Nobes, D. C., Ferguson, R. J., Brierley, G. J., 2001. Ground-Penetrating Radar and Sedimentological Analysis of Holocene Floodplains: Insight from the Tuross Valley, New South Wales. *Australian Journal of Earth Sciences*, 48: 347–355

Saarenketo, T., Scullion, T., 2000. Road Evaluation with Ground Penetrating Radar. *Journal of Applied Geophysics*, 43: 119–138

Shapira, A., Hofstetter, A., 1993. Source Parameters and Scaling Relationships of Earthquakes in Israel. *Tectonophysics*, 217: 217–226

Smith, D., 1986. Application of the Pole-Dipole Resistivity Technique to the Detection of Solution Cavities beneath Highways. *Geophysics*, 51: 833–837

Taner, M. T., Koehler, F., 1969. Velocity Spectra-Digital Computer Derivation and Applications of Velocity Functions. *Geophysics*, 34: 859–881

van Leeuwen, T., Mulder, W. A., 2008. Velocity Analysis Based on Data Correlation. *Geophysical Prospecting*, 56: 791–803

van Overmeeren, R., 1998. Radar Facies of Unconsolidated Sediments in the Netherlands: A Radar Stratigraphy Interpretation Method for Hydrogeology. *Journal of Applied Geophysics*, 40: 1–18

Vaughan, C., 1986. Ground-Penetrating Radar Surveys Used in Archaeological Investigations. *Geophysics*, 51: 595–604

Wolf, L., Collier, J., Tuttle, M., et al., 1998. Geophysical Reconnaissance of Earthquake-Induced Liquefaction Features in the New Madrid Seismic Zone. *Journal of Applied Geophysics*, 39: 121–129

Yilmaz, O., 1987. Seismic Data Processing. Society of Exploration Geophysics, Tulsa. 525

Zain Eldeen, U., Delvaux, D., Jacobs, P., 2002. Tectonic Evolution in the Wadi Araba Segment of the Dead Sea Rift, Southwest Jordan. *EGU Stephan Mueller Special Publication Series*, 2: 63–81